Journal of Photochemistry & Photobiology, B: Biology 241 (2023) 112672

Contents lists available at ScienceDirect

Journal of Photochemistry & Photobiology, B: Biology

journal homepage: www.elsevier.com/locate/jphotobiol

Antimicrobial 405 nm violet-blue light treatment of ex vivo human platelets leads to mitochondrial metabolic reprogramming and potential alteration of Phospho-proteome

Sirsendu Jana [a,*], Michael R. Heaven [a,1], Neetu Dahiya [a], Caitlin Stewart [b], John Anderson [b], Scott MacGregor [b], Michelle Maclean [b,c], Abdu I. Alayash [a], Chintamani Atreya [a,*]

[a] Office of Blood Research and Review, Center for Biologics Evaluation and Research, Food and Drug Administration, Silver Spring, MD 20993, USA
[b] The Robertson Trust Laboratory for Electronic Sterilization Technologies, Department of Electronic and Electrical Engineering, University of Strathclyde, Glasgow, United Kingdom
[c] Department of Biomedical Engineering, University of Strathclyde, Glasgow, United Kingdom

ARTICLE INFO

Keywords:
Pathogen reduction technologies: 405 nm light
Platelets
Bioenergetics
Mitochondria
Proteomics

ABSTRACT

Continued efforts to reduce the risk of transfusion-transmitted infections (TTIs) through blood and blood components led to the development of ultraviolet (UV) light irradiation technologies known as pathogen reduction technologies (PRT) to enhance blood safety. While these PRTs demonstrate germicidal efficiency, it is generally accepted that these photoinactivation techniques have limitations as they employ treatment conditions shown to compromise the quality of the blood components. During ex vivo storage, platelets having mitochondria for energy production suffer most from the consequences of UV irradiation. Recently, application of visible violet-blue light in the 400–470 nm wavelength range has been identified as a relatively more compatible alternative to UV light. Hence, in this report, we evaluated 405 nm light-treated platelets to assess alterations in energy utilization by measuring different mitochondrial bioenergetic parameters, glycolytic flux, and reactive oxygen species (ROS). Furthermore, we employed untargeted data-independent acquisition mass spectrometry to characterize platelet proteomic differences in protein regulation after the light treatment. Overall, our analyses demonstrate that ex vivo treatment of human platelets with antimicrobial 405 nm violet-blue light leads to mitochondrial metabolic reprogramming to survive the treatment, and alters a fraction of platelet proteome.

1. Introduction

Current pathogen reduction technologies (PRTs) for ex vivo stored human blood and blood components were developed to reduce or inactivate infectious agents present in the blood supply. This included solvent/detergent methods for human plasma or, ultraviolet (UV) light-based methods for stored plasma, platelets, and red blood cells prior to transfusion. The advantages and disadvantages of these technologies were recently reported in a Food and Drug Administration (FDA) workshop proceedings (1). While PRTs are effective against the pathogens, UV light-based technologies especially have demonstrated unintended consequences on the quality of the treated transfusion products which has been comprehensively reviewed (2). Hence, the field of PRT is open to improvements as the ideal PRT would be relatively inexpensive, simple to implement and, with no or minimal effect on the quality or efficacy of the transfusion product (3).

Because antimicrobial UV light is known to cause adverse effects on the treated products, application of visible violet-blue light in the 400–470 nm wavelength range has been identified as a relatively safer alternative. For example, several studies have demonstrated the antimicrobial potential of visible violet-blue light in clinical medicine and public health (4). Violet-blue light-based pathogen inactivation in clinical contexts can be achieved at lower doses of light relative to the dose levels required to cause damage to human cells (4). Based on the available comprehensive experimental evidence, towards identifying the “ideal PRT”, we have been evaluating high intensity narrow spectrum (HINS) 405 nm violet-blue light that falls within the visible light spectrum as a potential technology for pathogen inactivation in blood

* Corresponding authors.
E-mail addresses: sirsendu.jana@fda.hhs.gov (S. Jana), chintamani.atreya@fda.hhs.gov (C. Atreya).
[1] Present address: Vulcan Biosciences, Inc., 1500 1st Ave North, Birmingham, AL 35203, USA.

https://doi.org/10.1016/j.jphotobiol.2023.112672
Received 5 October 2022; Received in revised form 16 February 2023; Accepted 18 February 2023
Available online 21 February 2023

and blood components. To date, we have successfully demonstrated this light as a pathogen reduction tool or antimicrobial agent for human plasma and, platelets stored in plasma, by experimentally contaminating the two blood components with a number of bacteria (5–7), feline calicivirus (FCV), Human immunodeficiency virus (HIV)-1 (8,9) and a blood-borne protozoan parasite *Trypanosoma cruzi* (10). In most of these studies, a 405 nm light dose of 270 J/cm^2 has been identified to be sufficient to reduce pathogens while not harming the quality of the treated blood component(s).

Platelets stored in plasma treated with 405 nm light behave similar to the light-untreated samples both in vitro (10) and in vivo in a severe combined immunodeficient (SCID) mouse model (6). Since antimicrobial action of 405 nm light involves generation of reactive oxygen species (ROS), we have previously evaluated this light effect on plasma protein integrity and possible advanced oxidation protein products (AOPP) and demonstrated that 405 nm violet blue light-treated human plasma does not show any visible degradation of proteins, nor does it produce AOPPs measured by Chloramine-T based AOPP assay, at the light doses that effectively inactivate pathogens (7).

In this report, we evaluated 405 nm light-treated platelets to assess alterations in platelet energy utilization, overall effects on mitochondrial respiratory function, and protein regulation differences with an untargeted quantitative proteomics platform.

2. Material and Methods

2.1. Collection of Platelets from Healthy Human Donors and 405 Nm Light Treatment of Platelets

Apheresis collected human platelet concentrates from each donor split into two transfer bags containing equal volume of platelets were obtained from the National Institutes of Health Blood Bank (Bethesda, MD, USA). After overnight storage at 22 ± 2 °C under agitation, for each experiment, one platelet bag was used as control (no light treatment) and the other bag was used for the light treatment so that single donor platelets were paired for each experiment to avoid donor-to-donor variation within the experiment; platelets in the bags were exposed to 405 nm light, at an irradiance of approximately 15 mW/cm^2, for 1 h (= light dose 54 J/cm^2), 3 h (= light dose 216 J/cm^2), and 5 h (= light dose 270 J/cm2). For recovery studies, control, and light treated platelets for 5 h were incubated in the platelet shaker after the treatment and examined at 24 h. Exposure to 405 nm light was performed in an incubator shaker (US Patent Application no. 62/236, 706, 2015), equipped with a light source composed of narrowband 405 nm LED arrays (FWHM ~20 nm; LED Engin, CA, USA). All experiments were done at 22 ± 2 °C under shaking conditions (72 rpm). Study involving human subjects' protocol was approved by FDA Research Involving Human Subjects Committee (RIHSC, Exemption Approval #11-036B).

2.2. Biochemical Characterization of Ex Vivo Stored Platelets

Platelets were counted using the pocH-100i hematology analyzer (Sysmex, Kobe, Japan) as per manufacturers' instructions. Effect of 405 nm light on biochemical parameters such as pH, lactate, glucose, partial carbon dioxide and oxygen pressure, potassium and chloride levels were compared using a Start Profile CCS Time Blood Gas Analyzer (Nova Biomedical, Waltham, MA, USA).

2.3. Mitochondrial Bioenergetic, Glycolytic Flux, and Superoxide Measurements

To measure mitochondrial respiratory function and glycolytic function in platelets, oxygen consumption rate (OCR) and extracellular acidification rate (ECAR) were assessed respectively in real-time using an Extracellular Flux (XF24) analyzer (Agilent Seahorse, Santa Clara, CA, USA) following a protocol described before (11). Briefly, 1.5 × 10^7 platelets were plated in each well of a 24-well XF-V7 cell culture plate (Agilent-Seahorse) as per a previously published protocol (12,13). All the mitochondrial OXPHOS assays were done using XF-assay media (Agilent-Seahorse) supplemented with 10 mM glucose, 5 mM pyruvate and 2 mM glutamate. Mitochondrial OCR was assessed under different bioenergetic states e.g. coupled, uncoupled and inhibited states created by automated sequential injections of oligomycin (2 μM), carbonyl cyanide-p-trifluoro-methoxyphenylhydrazone (FCCP, 2 μM) and a combination of mitochondrial inhibitors (rotenone, 1 μM and antimycin A, 1 μM) respectively (11). Similarly, platelet's glycolytic capacity was assessed by ECAR experiments, where a glucose free XF-assay medium was used. Real time glycolytic profile was obtained by sequential addition of glucose (10 mM), oligomycin (1 μM) and glycolytic inhibitor 2-deoxyglucose (2-DG, 100 mM) to the wells.

The OCR and ECAR values were plotted using XF24 software, version 1.8. To eliminate any background OCR or ECAR, a few blank wells with only XF assay media were also run. Various bioenergetic and glycolytic parameters were calculated following manufacturer's protocol and as described earlier (13,14). Briefly, basal respiration was considered as the difference between maximum OCR obtained before oligomycin addition and non-mitochondrial OCR obtained after rotenone/antimycin A whereas the maximal respiration was the difference between maximum OCR induced by FCCP and non-mitochondrial OCR. ATP-linked respiration was calculated from the difference in OCR recorded before and after the oligomycin addition to get the complex V/ATP synthase activity. Similarly, glycolysis was considered as the maximum ECAR obtained after addition of glucose and the glycolytic capacity was the maximum ECAR achieved by oligomycin addition that shuts down ATP generation oxidative phosphorylation. Glycolytic reserve was calculated from the difference between glucose-induced and oligomycin-induced rise in ECAR (11,14).

Mitochondrial superoxide generation in platelets was monitored by a Synergy HTX multimode plate reader (Biotek Instruments, Inc., Winooski, VT, USA) at 580 nm using a mitochondrial ROS-specific MitoSOX fluorescent dye (5 μM) (Thermo Fisher Scientific, Waltham, MA, USA) as described earlier (11).

2.4. Mass Spectrometry Sample Preparation

Fractionated platelet samples were placed in sodium dodecyl sulfide (SDS) to a final concentration of 1% (*v*/v). The platelets were homogenized and samples were boiled for 5 min at 99 °C and subjected to SDS-polyacrylamide gel electrophoresis (PAGE) for 5 min followed by an in-gel trypsin digestion with iodoacetamide alkylation as described earlier (15).

2.5. Micro-Data Independent Acquisition (μDIA) Mass Spectrometry

The peptide digests were analyzed by LC-MS/MS on a Fusion Lumos Orbitrap mass spectrometer (Thermo Fisher Scientific) in conjunction with an M-class HPLC (Waters, Milford, MA, USA). Peptides were separated using a 75 μm × 250 mm 2 μm C18 reverse phase analytical column (Thermo Scientific). Peptide elution was performed using an increasing percentage of acetonitrile over a 120-min gradient with a flow rate of 300 nL/min. The mass spectrometer was operated in data-independent acquisition (DIA) mode with MS2 spectra acquired at 53 distinct 10 *m/z* shifted mass windows stepping from 400 to 920 m/z with an MS survey scan obtained once every duty cycle from 390 to 930 m/z. MS and MS2 spectra were acquired with an Orbitrap scan resolution of 60,000 and 30,000, respectively. The accumulation gain control (AGC) was set to 1 × 10^6 and 1 × 10^5 ions with a maximum injection time of 50 and 45 milliseconds for MS and MS2 scans, respectively. The precursor ions in MS2 fragment ion scans were selected across a mass isolation window of 15 *m/z* and dissociated by HCD (High Energy Collisional Dissociation) with a 30% normalized collision energy.

2.6. μDIA Proteomic Data Analyses

Raw MS/MS spectra were analyzed using Protalizer μDIA software (v1.1.4.1) from Vulcan Biosciences (Birmingham, AL, USA) (16). Peptide and protein identifications were made using the Protein Farmer search engine against the human Swiss-Prot database (2020–11 release). Mass spectra were identified and quantified with a 12 ppm fragment ion mass tolerance after mass calibration. Carbamidomethylation of Cys residues was searched as a fixed modification in all analyses, and where indicated, the phosphopeptide potential modification search was performed at Ser, Thr, and Tyr amino acids. Peptides with one trypsin missed cleavage were included in the analysis. A strict false discovery rate (FDR) based on a reversed database search of 1% at the peptide level and 5% at the protein level was applied for each sample analyzed. Normalized peptide and protein quantitative relative abundance values were calculated by normalizing the MS2 chromatogram sum area intensity of each peptide to the total sum intensity of all peptide MS2 chromatograms in each sample followed by Log2 transforming the values and applying a two-tailed unpaired *t-test* as described previously (16). Peptide missing values (originally assigned zero) were inputted as the smallest quantified peptide MS2 chromatogram area in each sample.

2.7. Statistical Analyses

Statistical analysis was performed using Microsoft Excel. Unless otherwise indicated, statistical significance was calculated using Student's *t*-test for paired samples, where $P < 0.05$ was considered significant between groups. All data are presented as mean ± standard deviation (SD), at the 95% confidence level.

3. Theory and Calculation

Since, platelets utilize mitochondria-generated energy resources, protecting platelet mitochondria and their functions from oxidative damage should be a fundamental consideration in selecting any new pathogen inactivation methods for stored platelets or to improve the quality of platelets with existing PRTs (17). With this rationale, we evaluated platelets' mitochondria following 405 nm light treatment and also studied platelet proteome changes. Our results support for further evaluation of this technology to see whether it will serve as a pathogen reduction technology for ex vivo stored platelets preserved for transfusion.

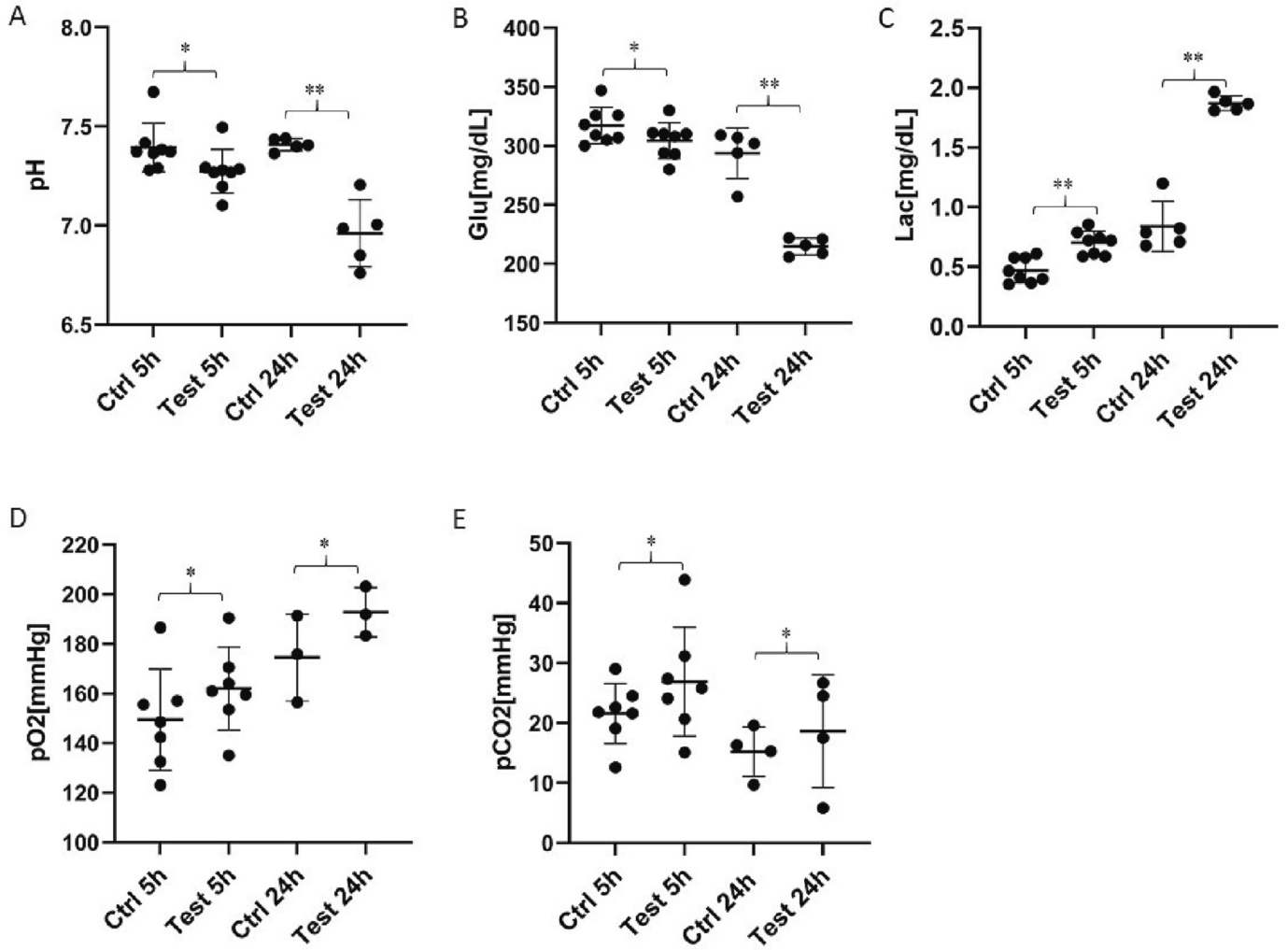

Fig. 1. In vitro Biochemical characterization of ex vivo stored platelets treated with 405 nm violet-blue light. Platelets were light exposed for 5 h (270 J/cm$^{2)}$ (Test 5 h) and compared to platelets with no light treatment for 5 h (Ctrl 5 h). (A) pH (B) Glucose level [Glu (mg/dL) (C) Lactate level [Lac (mg/dL) (D) Partial oxygen pressure [pO_2 (mmHg) (E) Partial carbon dioxide pressure [pCO_2 (mmHg)]. Each point represents the data from platelets obtained from different donors measured in at least three independent experiments. The 405 nm exposed samples relative to the control were analyzed by *t*-test. * not significant ($P > 0.05$); ** significant ($P < 0.05$). (For interpretation of the references to colour in this figure legend, the reader is referred to the web version of this article.)

4. Results

4.1. Effect of 405 nm Light on Platelet In Vitro Biochemical Parameters

A 405 nm light dose of 270 J/cm2 (i.e., 5 h treatment) on ex vivo stored platelets was evaluated by assessing the quality of platelets after 5 h light exposure followed by 24 h recovery in the platelet shaker (Fig. 1). Each metabolites measured were obtained from at least three independent experiments with different donors ($n = 3$). As platelets are metabolically active during storage, they utilize glucose and generate metabolites, such as lactate which causes a decrease in pH. A pH lower than 6.2 is known to negatively impact quality of the platelets. As seen in Fig. 1A, the difference in pH values between control platelets and platelets treated with the light for 5 h was not significant. While the difference in pH between non-treated platelets followed by 24 h recovery, and platelets treated with the light for 5 h followed by 24 h recovery, was statistically significant ($P = 0.0004$), it was still within the acceptable range of 7.0–7.4, in all tested samples. When results from 5 h control vs. 24 h control and 5 h test vs. 24 h test was considered, glucose levels decreased about 8% in controls and 30% in test samples, and lactate levels increased about 78% in controls and 168% in test samples (Fig. 1B and C). Other parameters such as oxygen pressure (Fig. 1D) and partial carbon dioxide (Fig. 1E) was statistically similar in control and test samples after 5 h treatment and at 24 h recovery period.

4.2. Effect of 405 nm Light Treatment on Bioenergetic Homeostasis in Ex Vivo Stored Platelets

To assess the energy utilization in platelets exposed to 405 nm light, we monitored both aerobic-mitochondrial bioenergetics and anaerobic-glycolytic proton flux in real time using an Extracellular Flux (XF) Analyzer (Agilent-Seahorse Bioscience). As a direct indicator of mitochondrial respiration, oxygen consumption rate (OCR) was measured from the platelets and plotted in real time to obtain a bioenergetic profile. Figs. 2 A-D show bioenergetic profiles of platelets treated with varying periods of 405 nm light ($n = 3$ human platelet samples analyzed). Different states of mitochondrial respiration were calculated from the OCR plots e.g., basal respiration, ATP-linked respiration, and maximal respiration (Fig. 2E). Light treatment for 1 h did not affect mitochondrial bioenergetic functions significantly, as all the measured bioenergetic indices remained unaffected. Light treatment for 3 h caused a detectable loss relative to 1 h treatment in maximal respiration. Although basal respiration and ATP-linked respiration were slightly diminished by 3 h light treatment, the values were not statistically significant compared to untreated controls. When platelets were exposed to 405 nm light for 5 h (270 J/cm^2), all the bioenergetic parameters were impacted significantly (Fig. 2E; $P < 0.05$).

In a similar experimental setup, we also assessed glycolytic rate by measuring the proton flux created by lactate produced through glycolysis. For this, we employed an XF analyzer to measure extra-cellular acidification rate (ECAR) as an indicator of glycolytic acidification in platelets. The ECAR values measured in real time were plotted to obtain glycolytic metabolic profile (Fig. 3 A-C). Basal glycolysis was induced by the addition of glucose which was not affected by treatment with 405 nm light for 1 h. We also calculated glycolytic capacity and glycolytic reserve in those cells. No changes in glycolysis were seen in platelets exposed to 405 nm light for 1 h when compared with untreated control platelets (Fig. 3A). However, platelets exposed to 405 nm light for 5 h led to a significant rise in both glycolysis and glycolytic capacity (Fig. 3B, $P < 0.05$). This observation is in agreement with the in vitro biochemical data presented in 4.1 and Fig. 1.

The 5 h exposure to 405 nm light caused almost 50% loss in basal and ATP-linked respiration at 5 h compared to untreated platelets, whereas the maximal respiration was diminished by 60%. Even after 24 h recovery following 5 h blue light treatment, both basal and ATP-linked respiration remained unchanged compared to the 5 h values. Surprisingly, less loss of maximal respiration was found at 24 h recovery time compared to 5 h treatment values, indicating a possible gain in mitochondrial respiratory reserve capacity by 24 h post-treatment, i.e., treated platelets were able to partially recover from the light insult. Maximal respiration was caused by a collapse of the proton gradient induced by the uncoupler (FCCP), resulting in an uninhibited flow of electrons through the respiratory chain complexes. Thus, leading to maximum oxygen consumption by cytochrome *c* oxidase (complex IV).

4.3. 05 nm Light Induces Mitochondrial Reactive Oxygen Species (ROS) that Can Be Mitigated by Mito-Q Antioxidant in Ex Vivo Stored Platelets

To understand the underlying mechanism of 405 nm light mediated impediment of mitochondrial bioenergetic function, we measured mitochondrial ROS production using a mitochondrial superoxide specific fluorescent probe MitoSOX. The 5 h light-treated platelets showed a significant rise in mitochondrial superoxide formation ($P < 0.01$), whereas 1 h treatment did not show any noticeable difference compared to untreated control platelets (Fig. 4A). We also performed an XF assay to measure mitochondrial oxygen consumption in the presence of two separate sets of antioxidants. The first set was comprised of general antioxidants e.g., *N*-acetyl cysteine (NAC) and D-mannitol, whereas the second set of antioxidants e.g., Mito-Tempol and Mito-Q, were more specific towards mitochondria carrying a lipophilic cation TPP+ which helps these compounds reach easily to mitochondria (18). When platelets were incubated with these antioxidants during 405 nm light exposure, only Mito-Q, a ubiquinone derivative was effective in mitigating the damage inflicted by the violet-blue light on mitochondrial functions as shown in the Fig. 4B. Although there was no significant difference found in basal respiration, Mito-Q showed a significant protection on ATP-linked respiration and maximal respiration when compared with 405 nm light treated platelets (Fig. 4B; $P < 0.05$). As a result of increased rate of glycolysis, glycolytic reserve capacity was also elevated significantly in the light treated platelets ($P < 0.05$). A more pronounced effect on glycolysis was seen following the 24 h post-treatment recovery period. A persistent rise in glycolytic activity in those platelets were possibly a compensatory effect for the deficiency of mitochondrial function.

4.4. Quantitative Proteomic Analysis of 405 Nm Light-Treated Ex Vivo Stored Platelets

To identify relative protein differences in platelets treated with 405 nm light, two sets of platelet samples were analyzed. The first set was platelets light-treated for 5 h and control platelets that were not subjected to the light treatment. The second set was platelets light-treated for 5 h followed by a 24 h recovery period and corresponding control platelets (n = 3 human platelet samples analyzed in all four experimental conditions). A database search of the resulting MS/MS tandem spectra allowed quantification of 1801 proteins across the samples corresponding to 17,215 peptides. We observed nine proteins to have lower quantitative levels in the 5 h treated versus control samples, and six proteins to have higher quantitative levels in the 5 h light-with 24 h recovery versus the corresponding control samples (minimum fold-change ±1.5 and $P < 0.05$). These differentially regulated proteins from both sets were then analyzed for their respective longitudinal abundance by expressing the (treatment/control) protein ratio per individual (Table 1). The entire protein quantification results are shown graphically (Fig. 5) and as a list (Supplemental Table 1). The nine proteins that demonstrated lower expression upon 270 J/cm^2 405 nm light treatment relative to the non-treated samples include: phosphatidylinositol 3-kinase catalytic subunit type 3 (PIK3C3), protein phosphatase 1 catalytic subunit gamma (PPP1CC), NADH:ubiquinone oxidoreductase core subunit V1 (NDUFV1), ankyrin 2 (ANK2), tubulin alpha like 3 protein (TUBAL3), ubiquitin-fold modifier conjugating enzyme 1 (UFC1), MTSS I-BAR domain containing 1 protein (MTSS1, beta actin

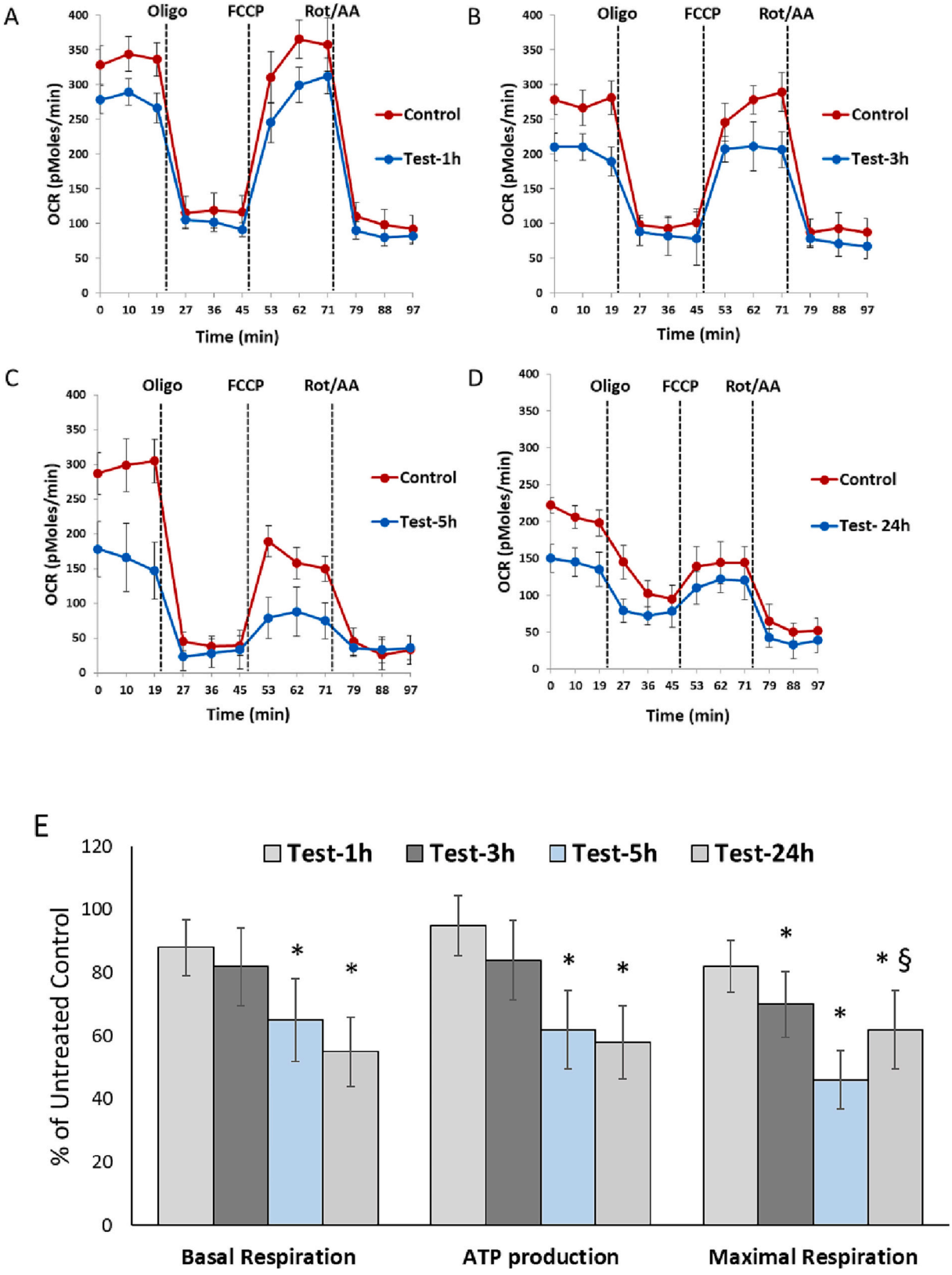

Fig. 2. 405 nm light induces mitochondrial dysfunction in platelets. Platelets were exposed to violet-blue light for 1 h, 3 h and 5 h (please refer to M & M for light dose equivalency). Mitochondrial OXPHOS activity was monitored in real time by plotting OCR in platelets with (Test) or without (Control) 405 nm light treatments for (A) 1 h, (B) 3 h, (C) 5 h and (D) 24 h recovery after 5 h treatment. (E) Various mitochondrial bioenergetic parameters were calculated from the OCR plots as described in the methods section. Values are means ($n = 4$) ± SEM; *$P < 0.05$ vs. respective untreated control, § $P < 0.05$ vs. corresponding 5 h treatment group. (For interpretation of the references to colour in this figure legend, the reader is referred to the web version of this article.)

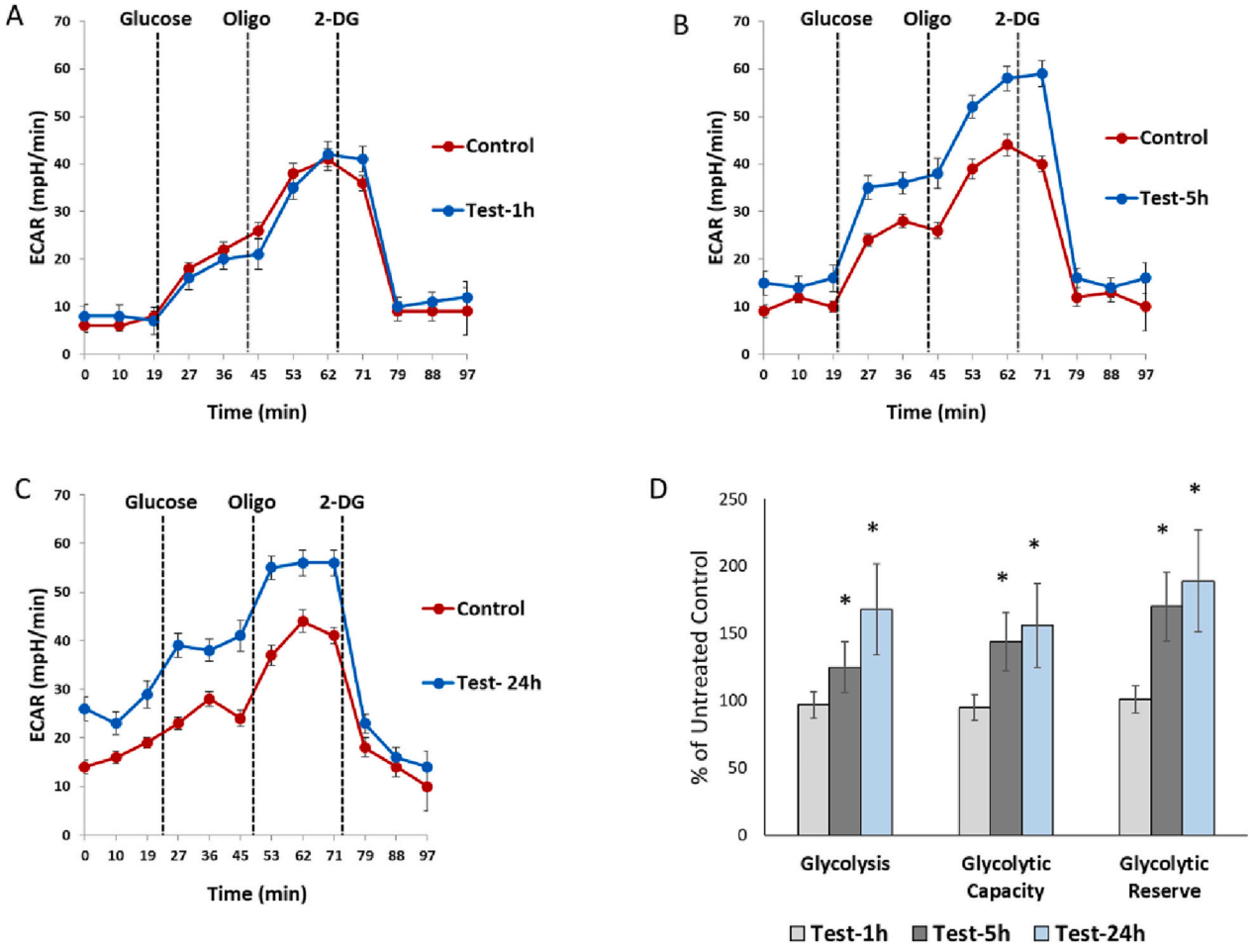

Fig. 3. 405 nm light induces glycolysis in platelets. Platelets were exposed to violet-blue light for 1 h, 3 h and 5 h (please refer to M & M for light dose equivalency). Glycolysis was monitored in real time by plotting ECAR in platelets with (Test) or without (Control) 405 nm light treatments for (A) 1 h, (B) 5 h and (C) 24 h recovery after 5 h treatment. (D) Various glycolytic parameters were calculated from the ECAR plots as described in the methods section. Values are means ($n = 4$) ± SEM; *$P < 0.05$ vs. respective untreated control values. (For interpretation of the references to colour in this figure legend, the reader is referred to the web version of this article.)

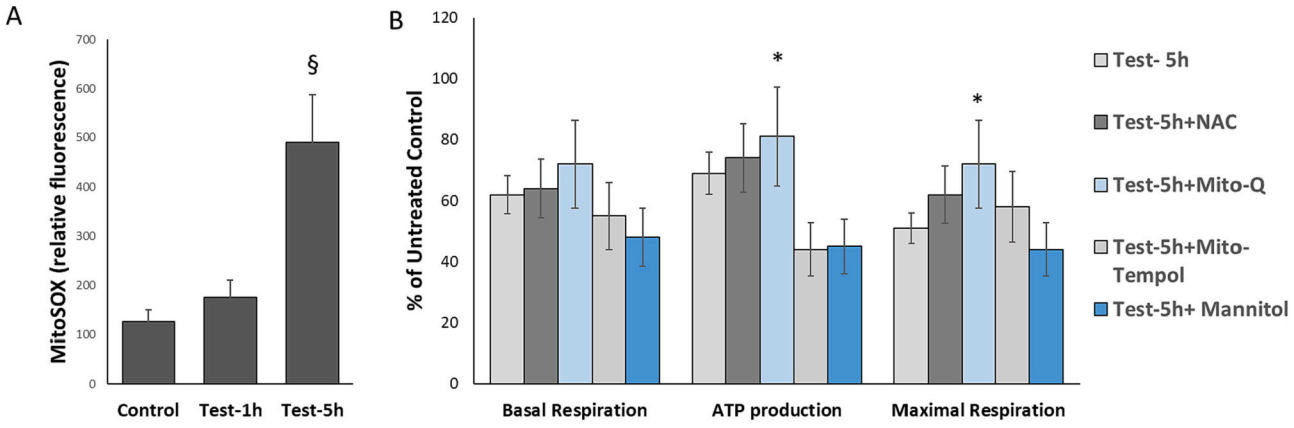

Fig. 4. 405 nm light produces mitochondrial reactive oxygen species in platelets and Mito-Q mitigates the effect. Platelets were exposed to violet-blue light for 1 h and 5 h and then mitochondrial superoxide production was measured using MitoSOX probe (A). Mitochondrial OXPHOS activity was monitored in real time by plotting OCR in platelets with (Test) or without (Control) 405 nm light treatments for 5 h in the presence or absence of various antioxidants as described in materials and methods (B) Various mitochondrial bioenergetic parameters were calculated from the OCR plots. Values are means ($n = 3$) ± SEM; § $P < 0.05$ vs. corresponding control; *P < 0.05 vs. corresponding 5 h treatment group. (For interpretation of the references to colour in this figure legend, the reader is referred to the web version of this article.)

Table 1
Fifteen out of 1801 quantified platelet proteins altered (minimum fold-change ±1.5 and P < 0.05) by 405 nm light treatment. Gene abbreviations correspond to Swiss-Prot assignments for each protein. Grey highlighted rows represent proteins quantitatively changed in the 5 h light-treated platelets relative to the controls and blue highlighted rows represent proteins quantitatively changed in the 5 h light treatment followed by 24 h recovery relative to the controls.

Gene/ Protein	Sample 1 (5 h treated/5 h control)	Sample 2 (5 h treated/5 h control)	Sample 3 (5 h treated/5 h control)	Sample 1 (5 h treated-24 h recovery/5 h no treatment-24 h recovery control)	Sample 2 (5 h treated-24 h recovery/5 h no treatment-24 h recovery control)	Sample 3 (5 h treated-24 h recovery/5 h no treatment-24 h recovery control)
PIK3C3	87.13	108.09	66.67	15.77	1.39	0.73
PPP1CC	2.98	3.90	2.86	1.38	1.15	0.68
NDUFV1	2.61	1.58	1.28	0.81	1.38	0.58
ANK2	1.75	3.74	2.72	0.84	0.45	0.82
TUBAL3	5.92	2.92	3.67	1.34	0.50	0.84
UFC1	4.46	2.24	5.05	1.97	0.93	0.46
MTSS1	10.29	1.18	4.79	8.71	0.69	0.66
ACTB	0.48	0.67	0.73	0.55	1.20	0.79
APOA4	0.35	0.94	0.46	0.78	1.06	0.27
HP	3.02	1.16	1.93	2.57	1.87	1.57
DENND3	1.23	0.52	1.32	2.59	2.19	1.38
PSMD1	2.55	0.97	1.39	1.34	1.69	1.84
TOLLIP	0.21	15.58	0.06	0.13	0.09	0.11
TANGO2	0.39	1.32	8.04	0.18	0.04	0.05
SURF4	0.93	1.53	1.75	0.50	0.62	0.52

(ACTB), and apolipoprotein A4 (APOA4). The six proteins that showed increased expression in platelets following 405 nm exposure (270 J/cm^2) and 24 h recovery include DENN domain containing 3 protein (DENND3), proteasome 26S subunit, non-ATPase 1 (PSMD1), toll interacting protein (TOLLIP), Transport and Golgi organization 2 homolog protein (TANGO2), surfeit 4 protein (SURF4) and haptoglobin (HP).

Next, we evaluated our data to determine if the violet-blue light stimulates any protein phosphorylation by performing a phosphopeptide query at Ser, Thr, and Tyr residues in our proteomic data (Supplemental Table 2). In total, our data search identified ten proteins with increased phosphorylation in the 5 h treated platelets compared to 5 h controls, and seventeen proteins with increased phosphorylation in the 5 h treated platelets followed by 24 h recovery compared to the respective controls (Table 2; minimum fold-change ±1.5 and $P < 0.05$). These 27 hyperphosphorylated proteins include: actin, actin-like protein and talins (ACTA2, ACTB, ACTBL2, TLN-1, TLN-2), fibrinogen gamma chain (FGG), beta arrestin-1 (ARRB1), MAGUK p55 scaffold protein 1 (MPP1), myosin heavy chain 9 and 11 (MYH3, MYH11), Guanine nucleotide-binding protein beta subunit −3 (GNB3), collagen type VIII alpha 2 chain (COL8A2), ubiquitin associated and SH3 domain containing B (UBASH3B), collagen type IV alpha 1 chain (COL4A1), collagen type VI alpha 3 chain (COL6A3), hypoxia up-regulated 1 protein (HYOU1), enolase 2 (ENO2), dynamin 1 like protein (DNM1L) and albumin (ALB).

5. Discussion

Generally, our results demonstrate that many of the in vitro quality parameters that we have tested were not significantly altered due to 405 nm light treatment of platelets including the pH, which remained within the acceptable range of 7–7.4, suggesting that the light treatment may not contribute to the pH associated platelet storage lesion; there was a substantial reduction in glucose levels and increase in lactate production (product of glycolysis) in platelets subjected to 5 h light treatment followed by 24 h recovery (Fig. 1). It was noted in a previous study by others that Mirasol-PRT (riboflavin + UV-A) treatment of platelets also increased both glycolytic flux as well as respiratory/enzymatic mitochondrial activity (19). Our analysis revealed that platelet's mitochondria generate ROS due to the light treatment and by switching to glycolytic pathway, able to sustain the insult caused by 405 nm light exposure for 5 h. Mitochondrial ROS production is a direct indicator of respiratory electron transport chain dysfunction. Further we have shown that the ROS effects in the light-treated platelet mitochondria can be mitigated by external supplementation of a mitochondrially-targeted antioxidant Mito-Q, suggesting that addition of this antioxidant as an adjunct prior to or during the light treatment may improve the platelet quality during storage. Nonetheless, in our previous report using a SCID mouse model we demonstrated that the survival and recovery of 405 nm light-treated and -untreated human platelets were statistically similar, suggesting that in vitro effects of 405 nm light treatment on platelets are recoverable and perhaps mitigated in vivo in the mouse. Based on this, we rationalize that supplementation of Mito-Q during the light treatment would certainly enhance the quality of the treated platelets during storage, while the light treatment was able to effectively reduce the bacterial contamination in the treated platelets (6). This observation was also corroborated in another study by others where 405 nm light selectively inactivated microbes in contaminated mouse platelets, and treated platelets behaved similar to control upon infusion into mice (20).

It is worth noting here that in the context of pathogen reduction in platelets stored in plasma, based on our observation that 405 nm light induces platelet mitochondrial ROS (mtROS), while it can be mitigated by supplementing a potent mitochondrial antioxidant to protect platelets, it is plausible that the platelet-mtROS serves as an additional ROS contributor to the well-established ROS-mediated antimicrobial effects driven by photoexcitation of either endogenous (present within the microbe) or, exogenous (present in the biological medium surrounding the microbe) photosensitizers such as porphyrins and flavins (4,8,21). Thus, in platelets stored in plasma, perhaps the two sources of ROS might be working in synergy to effectively inactivate pathogens present in the product as evidenced by our previous reports (6,9,10).

Our platelet proteomic analyses showed a quantitative perturbance in 15 proteins out of 1801 proteins quantified (0.835%), suggesting minimal number of proteins underwent changes in expression or turnover rate in the light-treated platelets relative to the untreated controls. This observation corroborates our previous study, which showed that 405 nm light treatment even at a higher light dose of 360 J/cm^2 did not produce advanced oxidation protein products in plasma which is the medium for ex vivo platelet storage (7). With regards to our analyses of phosphorylation status of 405 nm light-treated platelet proteins as an indicator of activation of platelet signaling pathways (i.e., phosphoproteome analysis), we observed only 27 proteins (10 proteins in 5 h light-treated and 17 proteins in 5 h light-treated followed by 24 h recovery, Table 2) appear to have undergone hyperphosphorylation due to the light exposure. While a small number of proteins have shown altered levels, and a few have undergone hyperphosphorylation, it is plausible that if phosphorylation states are stable over longer periods of platelet storage, that could affect platelet function through known and yet unknown mechanisms. For example, Talin-1 and -2 can be speculated to have direct effects on platelet integrin activation, and increased beta

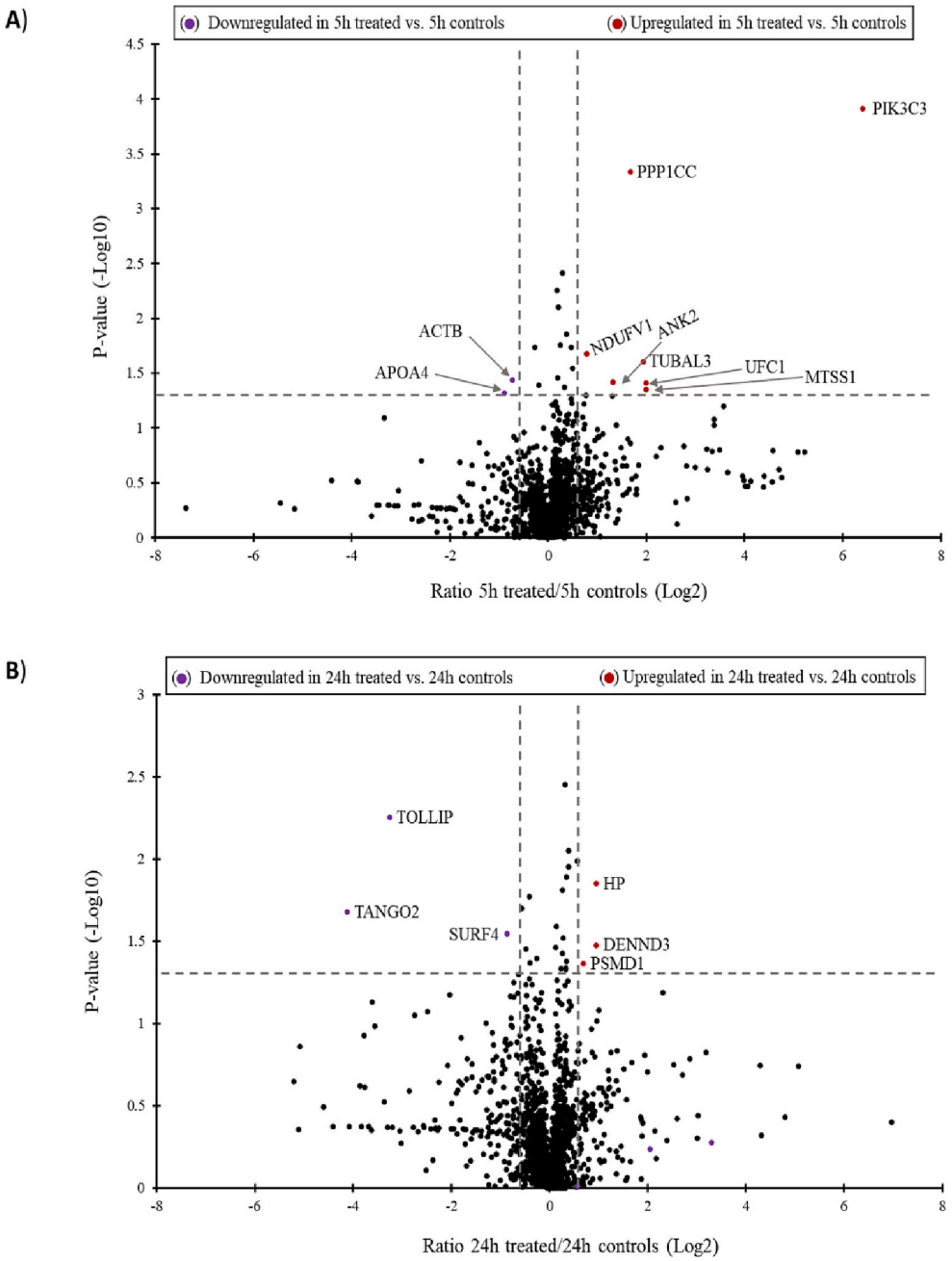

Fig. 5. 405 nm light treatment causes minimal perturbation in the platelet proteome. Data shown are untargeted quantification results from 1801 proteins quantified by μDIA mass spectrometry in the 5 h treated versus 5 h controls (A) and 5 h light treatment followed by 24 h recovery versus 5 h without light treatment followed by 24 h recovery controls (B). Upregulated proteins are shown in red and downregulated proteins are displayed in purple with Swiss-Prot gene abbreviations. The vertical lines denote fold-change values of −1.5 and 1.5 (without Log2 transformation), while the horizonal line shows a *P*-value of 0.05 (without -Log10 transformation). (For interpretation of the references to colour in this figure legend, the reader is referred to the web version of this article.)

arrestin-1 may alter the homeostatic surface levels of GPCR platelet receptors. Taken together these events in theory, may cause major impact on platelet reactivity. Another protein that was identified in this report is P13K3C3, the single isoform of the class III PI3K, also known as PI3KC3 or VPS34 (vacuolar protein sorting 34), which regulates platelet activation by affecting NADPH oxidase (NOX) assembly (22). Nonetheless, the observations reported here on the light-treated platelet phospho-proteome provides an opportunity in the future to study functional relevance of these hyperphosphorylated forms of proteins in platelet biology and certainly this area warrants further evaluation.

Prior proteomic studies to understand the effect of pathogen reduction based on Mirasol-PRT treatment, amotosalen hydrochloride + UV-A treatment and UV-C treatment pointed towards the induction of platelet morphology changes, alterations in intracellular platelet activation pathways or platelet shape and aggregation (23). In our treatments of platelets with 405 nm light, we observed that actin (ACTB) was downregulated similar to the reports with Mirasol-PRT treatment (24). Further, our light treated platelet proteomic data agrees with previous observations that the number of altered proteins due to the treatment is low in comparison with the whole proteome, and most proteins remain unimpacted by the treatments (23).

Finally, one intriguing observation that our proteomic analysis captured was the considerable elevation of haptoglobin (Hp) in platelets treated for 5 h with 405 nm light followed by 24 h recovery period. As Hp is a potent antioxidant and protects cells from oxidative stress (25), we hypothesize that the elevated platelet Hp levels observed in our study in response to 405 nm light could be the platelet's protective response to mtROS triggered by the light exposure. This is reminiscent of an early proteomic experimental observation in which it was noted that Hp and other proteins were found localized in activated platelets in human atherosclerotic lesions (26). This hypothesis is somewhat supported by our observation that there was less loss of maximal respiration after 24 h

Table 2
Platelet phosphopeptides altered either in the 5 h treatment and 24 h recovery or 5 h no treatment and 24 h recovery (control) or 5 h light treatment and 5 h no light treatment (minimum fold-change ±1.5 and $P < 0.05$) by 405 nm light. Gene abbreviations correspond to Swiss-Prot assignments for each protein, and the underlined amino acid in the peptide sequence shows the location of the phosphorylated residue(s). All C residues were detected with carbamidomethylation.

Phospho-Site location in the protein peptide	Peptide sequence	5 h treated-24 h recovery/ controls	P-value 5 h treated-24 h recovery/ controls	5 h-treated/ controls	P-value 5 h
T67 ACTBL2	GVLTLKYPIEHGVVTNWDDMEK	0.03	4.41E-01	142.64	7.61E-05
T321 HSD17B4	IDSEGGVSANHTSRATSTATSGFAGAIGQK	1.38	3.90E-01	0.01	1.80E-04
T105 ACTA2	VAPEEHPTLLTEAPLNPK	0.73	9.54E-01	45.84	2.07E-04
S125 FGG	MLEEIMKYEASILTHDSSIR	1.08	8.78E-01	19	3.44E-04
T350 ARRB1	GGLLGDLASSDVAVELPFTLMHPKPK	0.38	4.30E-01	0.07	7.46E-04
S344 MPP1	NISANEFLEFGSYQGNMFGTK	0.68	7.91E-01	0.06	1.27E-02
T873 MYH9	QLAAENRLTEMETLQSQLMAEK	0.45	9.88E-01	0.01	1.28E-02
T65 GNB3	IYAMHWATDSKLLVSASQDGK	0.12	3.28E-02	24.21	2.15E-02
Y364 ACTA2	QEYDEAGPSIVHR	0.81	4.37E-01	0.04	3.61E-02
S295 COL8A2	GEPGAVGPKGPPGVDGVGVPGAAGLPGPQGPSGAK	0.77	6.08E-01	0.13	5.00E-02
S75 UBASH3B	SVQAACDWLFSHVGDPFLDDPLPR	108.82	3.48E-05	1.75	3.32E-01
S1086 COL4A1	GEKGSIGIPGMPGSPGLK	52.81	7.30E-05	35.21	1.70E-01
S2829 COL6A3	LLPSFVSSENAFYLSPDIR	0.05	8.78E-05	11.06	2.68E-01
Y421 and S427 HYOU1	NINADEAAAMGAVYQAAALSK	90.72	9.60E-05	0.78	9.92E-01
T194 ACTB	ILTERGYSFTTTAER	392.11	2.70E-04	0	1.39E-01
Y1737 TLN1	VSQMAQYFEPLTLAAVGAASK	33.01	5.90E-04	0.75	4.99E-01
S1376 MYH9	MEDSVGCLETAEEVKR	2.53	1.15E-02	0.82	5.36E-01
Y54 and S61 ACTBL2	HQGVMVGMGQKDCYVGDEAQSK	0.56	1.38E-02	2.32	2.73E-01
S1408 TLN2	VLGESMAGISQNAK	2.45	1.68E-02	0.64	3.45E-01
S336 HSPH1	IEVPLYSLLEQTHLKVEDVSAVEIVGGATR	1.57	1.71E-02	1.04	9.24E-01
Y71 ACTA2	YPIEHGIITNWDDMEK	0.08	2.07E-02	1.25	8.21E-01
S990 and S992 TLN1	GSQAQPDSPSAQLALIAASQSFLQPGGK	0.13	2.77E-02	0.41	3.19E-01
S1518 MYH11	AEMEDLVSSKDDVGK	0.25	2.82E-02	1.03	8.36E-01
S115 ENO2	FGANAILGVSLAVCKAGAAER	1.82	2.87E-02	1.31	4.13E-01
T65 GNB3	IYAMHWATDSKLLVSASQDGK	0.12	3.28E-02	24.21	2.15E-02
S380 and T389 DNM1L	TLESVDPLGGLNTIDILTAIR	0.58	3.53E-02	1.67	3.48E-01
S328 ALB	SHCIAEVENDEMPADLPSLAADFVESKDVCK	3.62	4.77E-02	0.42	7.34E-01

recovery time compared to immediately after 5 h light treatment, indicating a possible gain in mitochondrial respiratory reserve capacity by 24 h post-treatment recovery with concurrent elevation of Hp. However, future experimental studies are warranted to test this hypothesis.

Since results reported here for the first time provided basic understanding of how platelets and mitochondria are responding to the light treatment, it provides an opportunity in the future to study the long-term effects of the light-induced ROS and phosphor-proteome alterations during the platelet storage period of 5–7 days as well as confirmation of protein changes such as protein expression and phosphorylation by orthogonal means.

In summary, our results reported here demonstrate that ex vivo treatment of platelets with 405 nm violet-blue light causes metabolic changes in platelets that are within the acceptable range of in vitro tests for platelets, reprograms mitochondrial metabolism for survival as a protective measure and the treatment-associated deleterious ROS induction is amenable to mitigation by antioxidant Mito-Q and, regulation of a small number of proteins in the context of larger platelet proteome was altered, as observed by others with other light-based PRTs. Overall, the results presented here and our previous report of 405 nm light-treated human platelet survival and recovery similar to non-treated control in a SCID mouse model together, lend support for further evaluation of 405 nm light technology to see whether it can serve as a safer alternative to UV light-based pathogen inactivation technologies for stored plasma and platelets.

Ethics statement

The studies involving human participants were reviewed and approved by FDA Research Involving Human Subjects Committee (RIHSC, Exemption Approval #11-036B). The patients/participants provided their written informed consent to participate in research studies as per NIH Blood Bank ethics guidelines and policies, which supplied human plasma used in this study.

Author contributions

SJ, ND, MH, CA and AIA designed the study. SJ, ND and MH performed the experiments, data analyses, and participated in writing of the manuscript and preparation of Figs. CA and AA reviewed the research plan, oversaw the project, analyzed data, and participated in developing the manuscript along with SJ, ND, and MH. CS, JA, SM and MM designed and constructed the 405 nm light device used in this study and participated in the review and editing of the manuscript. All authors contributed to the article and approved the submitted version.

Funding

This work was supported by FDA intramural research funds.

Declaration of Competing Interest

The authors have nothing to disclose.

Data availability

The original contributions presented in the study are included in the article. All inquiries can be directed to the corresponding authors.

Acknowledgements

This research work was conducted in the laboratories of CA and AA at the Center for Biologics Evaluation and Research, US Food and Drug Administration. Design and building of the light source were supported by Ruairidh Macpherson, Mark Wilson and technical staff at the Department of Electronic & Electrical Engineering, University of Strathclyde.

Appendix A. Supplementary data

Supplementary data to this article can be found online at https://doi.

org/10.1016/j.jphotobiol.2023.112672.

References

[1] C. Atreya, S. Glynn, M. Busch, S. Kleinman, E. Snyder, S. Rutter, et al., Proceedings of the Food and Drug Administration public workshop on pathogen reduction technologies for blood safety 2018 (commentary, p. 3026), Transfusion. 59 (9) (2019) 3002–3025.

[2] G. Escolar, M. Diaz-Ricart, J. McCullough, Impact of different pathogen reduction technologies on the biochemistry, function, and clinical effectiveness of platelet concentrates: an updated view during a pandemic, Transfusion. 62 (1) (2022) 227–246.

[3] P. Marks, N. Verdun, Toward universal pathogen reduction of the blood supply (conference report, p. 3002), Transfusion. 59 (9) (2019) 3026–3028.

[4] D. Haridas, C.D. Atreya, The microbicidal potential of visible blue light in clinical medicine and public health, Front. Med. (Lausanne). 9 (2022), 905606.

[5] M. Maclean, J.G. Anderson, S.J. MacGregor, T. White, C.D. Atreya, A new proof of concept in bacterial reduction: antimicrobial action of violet-blue light (405 nm) in ex vivo stored plasma, J. Blood Transfus. 2016 (2016) 2920514.

[6] M. Maclean, M.P. Gelderman, S. Kulkarni, R.M. Tomb, C.F. Stewart, J.G. Anderson, et al., Non-ionizing 405 nm light as a potential bactericidal Technology for Platelet Safety: evaluation of in vitro bacterial inactivation and in vivo platelet recovery in severe combined Immunodeficient mice, Front. Med. (Lausanne). 6 (2019) 331.

[7] C.F. Stewart, R.M. Tomb, H.J. Ralston, J. Armstrong, J.G. Anderson, S. J. MacGregor, et al., Violet-blue 405-nm light-based Photoinactivation for pathogen reduction of human plasma provides broad antibacterial efficacy without visible degradation of plasma proteins, Photochem. Photobiol. 98 (2) (2022) 504–512.

[8] R.M. Tomb, M. Maclean, J.E. Coia, E. Graham, M. McDonald, C.D. Atreya, et al., New proof-of-concept in viral inactivation: Virucidal efficacy of 405 nm light against feline Calicivirus as a model for norovirus decontamination, Food Environ. Virol. 9 (2) (2017) 159–167.

[9] V. Ragupathy, M. Haleyurgirisetty, N. Dahiya, C. Stewart, J. Anderson, S. MacGregor, et al., Visible 405 nm violet-blue light successfully inactivates HIV-1 in human plasma, Pathogens. 11 (7) (2022).

[10] K.I. Jankowska, R. Nagarkatti, N. Acharyya, N. Dahiya, C.F. Stewart, R. W. Macpherson, et al., Complete inactivation of blood borne pathogen Trypanosoma cruzi in stored human platelet concentrates and plasma treated with 405 nm violet-blue light, Front. Med. (Lausanne). 7 (2020), 617373.

[11] S. Jana, F. Meng, R.E. Hirsch, J.M. Friedman, A.I. Alayash, Oxidized mutant human Hemoglobins S and E induce oxidative stress and bioenergetic dysfunction in human pulmonary endothelial cells, Front. Physiol. 8 (1082) (2017).

[12] N. Cardenes, C. Corey, L. Geary, S. Jain, S. Zharikov, S. Barge, et al., Platelet bioenergetic screen in sickle cell patients reveals mitochondrial complex V inhibition, which contributes to platelet activation, Blood. 123 (18) (2014) 2864–2872.

[13] S. Ravi, B. Chacko, P.A. Kramer, H. Sawada, M.S. Johnson, D. Zhi, et al., Defining the effects of storage on platelet bioenergetics: the role of increased proton leak, Biochim. Biophys. Acta 1852 (11) (2015) 2525–2534.

[14] T. TeSlaa, M.A. Teitell, Techniques to monitor glycolysis, Methods Enzymol. 542 (2014) 91–114.

[15] M.B. Strader, S. Jana, F. Meng, M.R. Heaven, A.S. Shet, S.L. Thein, et al., Post-translational modification as a response to cellular stress induced by hemoglobin oxidation in sickle cell disease, Sci. Rep. 10 (1) (2020) 14218.

[16] M.R. Heaven, A.L. Cobbs, Y.W. Nei, D.B. Gutierrez, A.W. Herren, H. P. Gunawardena, et al., Micro-data-independent Acquisition for High-Throughput Proteomics and Sensitive Peptide Mass Spectrum Identification, Anal. Chem. 90 (15) (2018) 8905–8911.

[17] P. Gough, T. Getz, S. De Paoli, S. Wagner, C. Atreya, Analysis of the mechanism of damage produced by thiazole orange photoinactivation in apheresis platelets, Blood Transfus. 19 (5) (2021) 403–412.

[18] Q. Jiang, J. Yin, J. Chen, X. Ma, M. Wu, G. Liu, et al., Mitochondria-targeted antioxidants: a step towards disease treatment, Oxidative Med. Cell. Longev. 2020 (2020) 8837893.

[19] S.M. Picker, V. Schneider, L. Oustianskaia, B.S. Gathof, Cell viability during platelet storage in correlation to cellular metabolism after different pathogen reduction technologies, Transfusion. 49 (11) (2009) 2311–2318.

[20] M. Lu, T. Dai, S. Hu, Q. Zhang, B. Bhayana, L. Wang, et al., Antimicrobial blue light for decontamination of platelets during storage, J. Biophotonics 13 (1) (2020), e201960021.

[21] D.H. Kingsley, R.E. Perez-Perez, G. Boyd, J. Sites, B.A. Niemira, Evaluation of 405-nm monochromatic light for inactivation of Tulane virus on blueberry surfaces, J. Appl. Microbiol. 124 (4) (2018) 1017–1022.

[22] Y. Liu, M. Hu, D. Luo, M. Yue, S. Wang, X. Chen, et al., Class III PI3K positively regulates platelet activation and thrombosis via PI(3)P-directed function of NADPH oxidase, Arterioscler. Thromb. Vasc. Biol. 37 (11) (2017) 2075–2086.

[23] M. Prudent, A. D'Alessandro, J.-P. Cazenave, D. Devine, C. Gachet, A. Greinacher, et al., Proteome changes in platelets after pathogen inactivation—an Interlaboratory consensus, Transfus. Med. Rev. 28 (2014).

[24] C. Marrocco, A. D'Alessandro, G. Girelli, L. Zolla, Proteomic analysis of platelets treated with gamma irradiation versus a commercial photochemical pathogen reduction technology, Transfusion. 53 (8) (2013) 1808–1820.

[25] C.F. Tseng, C.C. Lin, H.Y. Huang, H.C. Liu, S.J.T. Mao, Antioxidant role of human haptoglobin, PROTEOMICS. 4 (8) (2004) 2221–2228.

[26] J.A. Coppinger, G. Cagney, S. Toomey, T. Kislinger, O. Belton, J.P. McRedmond, et al., Characterization of the proteins released from activated platelets leads to localization of novel platelet proteins in human atherosclerotic lesions, Blood. 103 (6) (2004) 2096–2104.